ISSN 1674-1056
http://cpb.iphy.ac.cn
http://iopscience.iop.org/cpb
中国物理 B
Chinese Physics
中国物理 Chinese Physics B

Electric field in two-dimensional complex plasma crystal: Simulated lattices

Behnam Bahadory
Citation: Chin. Phys. B . 2018, 27(2): 025202. **doi:** 10.1088/1674-1056/27/2/025202

Journal homepage: http://cpb.iphy.ac.cn; http://iopscience.iop.org/cpb

What follows is a list of articles you may be interested in

Rotation of a single vortex in dusty plasma

Jia Yan(闫佳), Fan Feng(冯帆), Fu-Cheng Liu(刘富成), Ya-Feng He(贺亚峰)
Chin. Phys. B . 2017, 26(9): 095202. **doi:** 10.1088/1674-1056/26/9/095202

Mode transition in dusty micro-plasma driven by pulsed radio-frequency source in C_2H_2/Ar mixture

Xiang-Mei Liu(刘相梅), Rui Li(李瑞), Ya-Hui Zheng(郑亚辉)
Chin. Phys. B . 2017, 26(4): 045202. **doi:** 10.1088/1674-1056/26/4/045202

Lower order three-dimensional Burgers equation having non-Maxwellian ions in dusty plasmas

Apul N Dev
Chin. Phys. B . 2017, 26(2): 025203. **doi:** 10.1088/1674-1056/26/2/025203

Plural interactions of space charge wave harmonics during the development of two-stream instability

Victor Kulish, Alexander Lysenko, Michael Rombovsky, Vitaliy Koval, Iurii Volk
Chin. Phys. B . 2015, 24(9): 095201. **doi:** 10.1088/1674-1056/24/9/095201

Dispersion relation and growth rate for a corrugated channel free-electron laser with a helical wiggler pump

A. Hasanbeigi, H. Mehdiank
Chin. Phys. B . 2013, 22(7): 075205. **doi:** 10.1088/1674-1056/22/7/075205

Electric field in two-dimensional complex plasma crystal: Simulated lattices

Behnam Bahadory†

Atomic and Molecular Department, Physics Faculty, Yazd University, Yazd 8915818411, *Iran*

(Received 3 September 2017; revised manuscript received 20 October 2017; published online 5 January 2018)

We focus on molecular dynamics simulated two-dimensional complex plasma crystals. We use rigid walls as a confinement force and produce square and rectangular crystals. We report various types of two-row crystals. The narrow and long crystals are likely to be used as wigglers; therefore, we simulate such crystals. Also, we analyze the electric fields of simulated crystals. A bit change in lattice parameters can change the internal structures of crystals and their electric fields notably. These parameters are the number of grains, grains charge, length, and width of the crystal. With the help of electric fields, we show the details of crystal structures.

Keywords: complex plasma, plasma crystal, free-electron laser

PACS: 52.27.Lw, 52.58.–c, 41.60.Cr **DOI:** 10.1088/1674-1056/27/2/025202

1. Introduction

Suspended macroscopic grains in plasma environment make it complex. The grains acquire a large quantity of negative charge and can form crystal inside a plasma. In laboratories, a lower electrode prevents grains from falling. Negative grains repel each other to infinity unless a confinement force makes them close together. In a typical experiment, a negative electrode plays the confinement force role.[1–4] Also, uniform grains with equal mass and spherical shape are very common.[5–9]

Conditions for crystallization is given by Coulomb coupling parameter:[10–13]

$$\Gamma = \frac{kq^2}{rk_{\mathrm{B}}T}\exp(-r/\lambda_{\mathrm{D}}), \tag{1}$$

where k is the Coulomb's constant, q is the grain charge, r is the intergrain distance, k_{B} is the Boltzmann constant, T is the temperature, and λ_{D} is the Debye length of the system. This means that if thermal energy is low and the Coulomb interaction (mainly charge of grains) is high, then lattice structures form. Complex plasma crystals are two-dimensional (2D) usually. Also, usually their lattices have hexagonal symmetry.[14–18]

In most papers, spring force is used as confinement force:[19–23]

$$\begin{cases} F_x = -k_x x, \\ F_y = -k_y y. \end{cases} \tag{2}$$

We use this assumption too.[24] When $k_x = k_y$, circular or hexagonal crystals are produced and when $k_x \neq k_y$, elliptical crystals are formed. In fact, only the repulsive nature of the force is important and any repulsive force can be used as a confinement force. We restrict this study to the 2D case and assume that grain levitation occurs at a definite height above the lower electrode in the plasma sheath due to the balance between grain weight and sheath field.[25–27] In the horizontal direction, there are two forces: screened Coulomb force and confinement force. The first force is formulated in the next section and rigid walls are used as the second confinement force. All crystals in this work are produced with the rigid wall boundaries. The geometry of the rigid walls is arbitrary, thus leading to the production of crystals with the same geometry. This simple technique is useful, specially for square, rectangle, and other right angle crystals.

Mirzanejhad and Bahadory[28] suggested an application for complex plasma crystals: they considered it as an electrostatic wiggler for free-electron laser, FEL. The FEL needs a long and strong transverse electric field. So, long complex plasma crystals with strong transverse electric field are better than a normal one for this purpose. In the present work, square, rectangle, and two-row crystals are simulated. These types of crystals can be long, and the transverse electric field of two-row crystals can be strong. We analyze the electric fields of these crystals and show that the electric fields of similar crystals differ a lot. Usually, crystals in laboratories are not complete and even small changes in grain positions leads to significant effects on the electric field in them. We discuss the effects of distance between rigid walls in two directions, grain number, and charge of each grain on the lattice type and number of rows in the crystals.

It must be noted that grain charge depends on the plasma parameters. For example, if plasma density or plasma temperature changes, grain charge will change. Sometimes, we use a normal quantity of grain charge and then we switch to another normal charge for comparison. We do not discuss experimen-

†Corresponding author. E-mail: Bahadory@yazd.ac.ir

© 2018 Chinese Physical Society and IOP Publishing Ltd

tal setup nor parameters that lead to a certain charge.

2. Crystals with arbitrary shape

In a complex plasma, each charged particle has a screened Coulomb potential:[29–33]

$$\varphi(r) = \frac{q}{r} \mathrm{e}^{-r/\lambda_\mathrm{D}}. \tag{3}$$

We use the x–y coordinate system for the 2D complex plasma crystal. If n grains exist in the plasma, the net force acting on the i-th grain is expressed as

$$\boldsymbol{F}_i = q^2 \sum_{j\neq i}^{n} \frac{\boldsymbol{r}_i - \boldsymbol{r}_j}{r_{ij}^3} \left(1 + \frac{r_{ij}}{\lambda_\mathrm{D}}\right) \mathrm{e}^{-r_{ij}/\lambda_\mathrm{D}}, \tag{4}$$

where $r_{ij} = |\boldsymbol{r}_i - \boldsymbol{r}_j|$.

Grains repel each other due to the force described in Eq. (4) but rigid wall boundaries exist. So the grains cannot escape; they regulate themselves and shape a crystal.

We use a molecular dynamics simulation. One of our purposes is to produce the crystals with arbitrary geometries and various sizes. In our simulations, grain charge, distance, and mass are normalized to electrons charge, Debye length, and grain mass respectively.

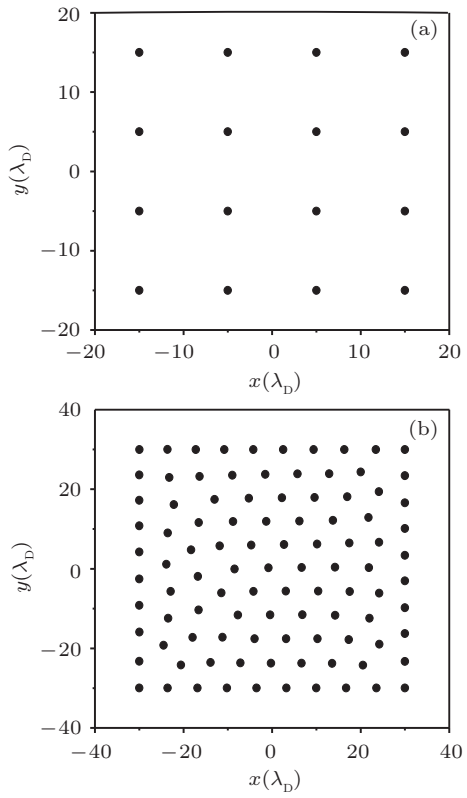


Fig. 1. Two square crystals. (a) $n = 16$, $q = 10^4 e$, $a = 30\lambda_\mathrm{D}$, and $b = 30\lambda_\mathrm{D}$. Inside structures are square. (b) $n = 100$, $q = 10^3 e$, $a = 60\lambda_\mathrm{D}$, and $b = 60\lambda_\mathrm{D}$. Only boundaries have a square shape and inside structures are hexagonal.

Figure 1 shows two square crystals. Number of grains, n, is chosen to be 16 and 100. In Fig. 1(a), size of square crystal is small and for this reason, grains form squares inside the crystal, too. Figure 1(b) shows that boundaries keep their effect on the edges of crystal but square structures do not exist inside the crystal. The crystal tends to reach the hexagonal lattice and inside structures of Fig. 1(b) have hexagonal symmetry. Similar results occur in any square crystal and rectangular shaped crystal. In general, geometrical boundaries form crystal contour and usually they are of short range.

By selecting different values of length a and width b, square crystals become rectangular. Figure 2 shows a rectangular crystal with 100 grains. In simulations, figure 2 is the same as Fig. 1(b) except the values of a and b, and in properties, both are similar.

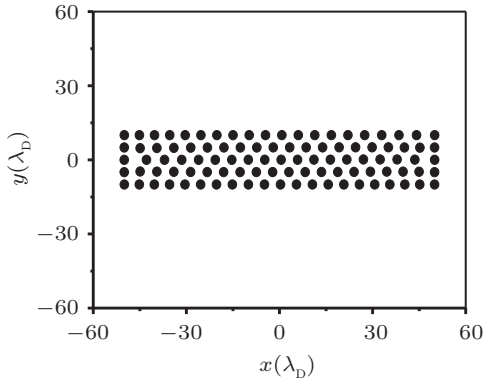


Fig. 2. A rectangular crystal with $n = 100$, $q = 10^3 e$, $a = 100\lambda_\mathrm{D}$, and $b = 20\lambda_\mathrm{D}$. Inside structures are hexagonal.

By increasing rectangle length and reducing its width, the number of grain rows decreases. With the help of simulation, we can predict suitable distances for obtaining particular cases, such as three-row grains in crystal. Factors that affect the number of rows are n, q, a, and b. By increasing n and q, the number of grain rows increases. For constant a, by increasing b the number of rows increases and conversely for constant b, by reducing a the number of rows increases. A rectangular crystal that has just two rows of grains is a two-row crystal. The two-row crystals are part of a hexagonal lattice and in ideal conditions, each grain is located in the middle of two grains in the top row and bottom row. We simulate two-row crystals by a different method from the method reported previously.[24] Rigid walls assumption that is used in the present work is simpler and surprisingly gives more complete crystals than by the previous method.

Figure 3 shows four two-row crystals but only one of them is perfect (approximately). In Fig. 3(a), the crystal characteristics are as follows: $n = 16$, $q = 10^4 e$, $a = 50\lambda_\mathrm{D}$, and $b = 8\lambda_\mathrm{D}$. In this crystal, grains of the top row are above the grains of the bottom row and hexagonal symmetry does not exist; like Fig. 1(a), large repulsive forces between grains overtake the short-range effect of boundaries and grains form square structures throughout the crystal. In other parts of Fig. 3, $q = 10^3 e$ and boundaries show their effects in short range, i.e., left and right ends only. The crystal shown in Fig. 3(b) has 9 grains in the top row and 11 grains in the bottom row. This situation represents the defect existing in the

crystal. This does not always occur, which is caused by the random initial positions of grains. Figure 3(c) shows a crystal that seems to be an ideal two-row crystal (except the left and right ends) but in the next section with the help of electric fields more details appear. the caption for figure 3 presents the characteristics of all crystals.

Except the length, figures 3(d) and 3(c) crystals are the same. The crystal shown in Fig. 3(d) does not have hexagonal symmetry and it has a structure between square and hexagonal, which is due to the small size of this crystal and the effect of right angle boundaries that attempt to give a square structure to near the area of the boundaries. In fact, the ideal two-row crystals are not easy to occur and in this case q, a, and b can change slightly, or sometimes, the value of n can change the internal structure of crystal notably.

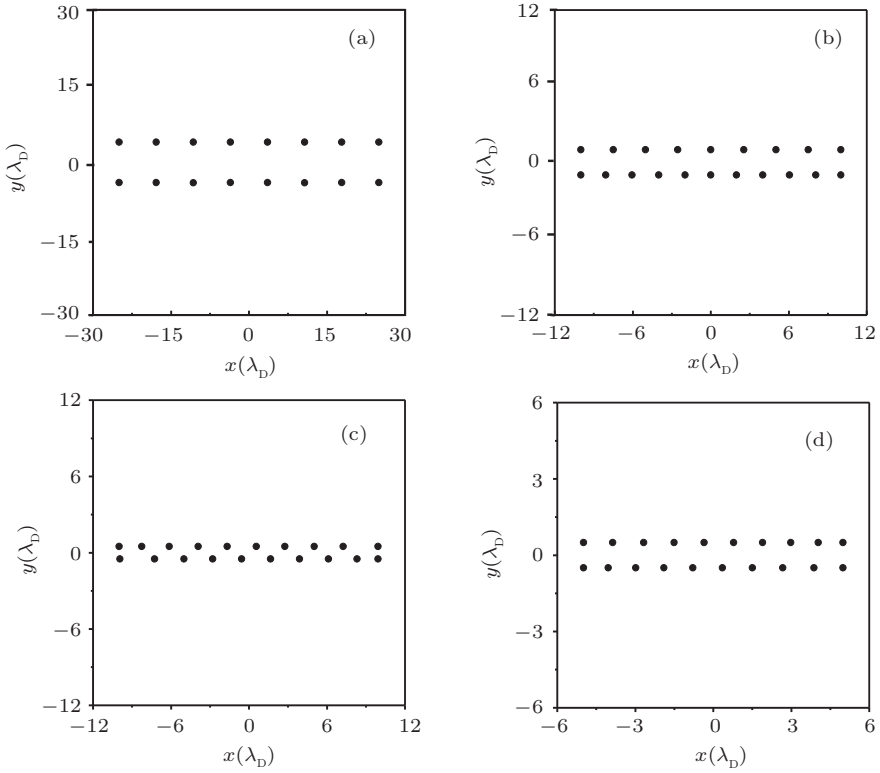


Fig. 3. Four two-row crystals with different structures. (a) $n = 16$, $q = 10^4 e$, $a = 50\lambda_D$, and $b = 8\lambda_D$, it is nearly the same as Fig. 1(a) and the grains have inside square structures. (b) $n = 20$, $q = 10^3 e$, $a = 20\lambda_D$, and $b = 2\lambda_D$, it has 9 grains in the top row and 11 grains in the bottom row. (c) $n = 20$, $q = 10^3 e$, $a = 20\lambda_D$, and $b = 1\lambda_D$. The grains have hexagonal structures. (d) $n = 20$, $q = 10^3 e$, $a = 10\lambda_D$, and $b = 1\lambda_D$, it is something between panels (a) and (c).

We are interested in long and narrow two-row crystals because they are suitable for FELs.[25] Narrow two-row crystals have strong transverse electric field that is essential for an electrostatic wiggler in FEL. On the other side, narrowing is equivalent to a small quantity of b, and small b leads to crystals with only one row. Our simulations are useful for predicting suitable conditions for the experimental setup. One of the long and narrow crystals is shown in Fig. 4. Its characteristics are as follows: $n = 100$, $q = 10^3 e$, $a = 70\lambda_D$, and $b = 2\lambda_D$. In this case there appears no hexagonal symmetry because grains in the top row are not between grains in the bottom row. In the next section, we analyze the electric fields of some simulated crystals including this crystal.

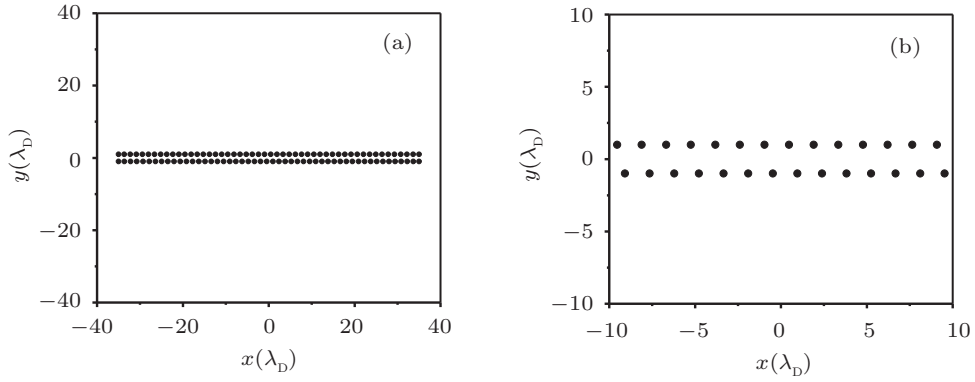


Fig. 4. (a) A long two-row crystal with $n = 100$, $q = 10^3 e$, $a = 70\lambda_D$, and $b = 2\lambda_D$. (b) Magnified middle part of panel (a), showing no existing hexagonal structure.

3. Electric fields inside crystals

In an ideal crystal, the frequency of longitudinal electric field E_x is twice the frequency of transverse electric field E_y; also the number of E_y peaks is equal to the number of grains in the crystal. The electric fields of crystals like those in Fig. 1(b) are not regular. Any little disordering at the grain position can make electric fields greatly irregular. Even crystals like the crystal in Fig. 2 that seems to have good fields, are not suitable for wigglers. Figure 5 shows the details of these crystal fields and asymmetries that cannot be seen easily from the grain positions. In each of all figures of this paper, an observation line for electric fields is in the middle of the crystal, i.e., $y = 0$.

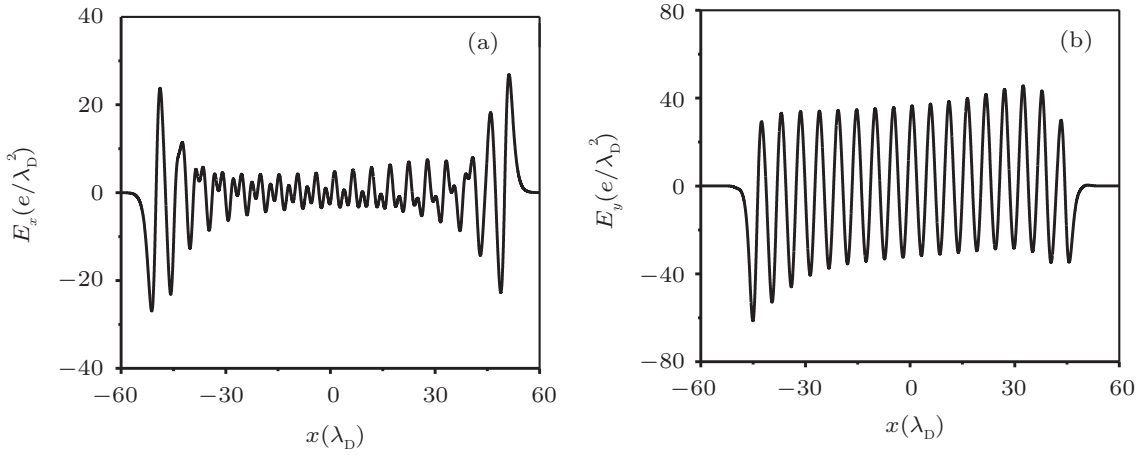


Fig. 5. (a) Longitudinal and (b) transverse electric fields in the middle of the crystal shown in Fig. 2 (at $y = 0$).

The electric field components E_x and E_y of the crystals shown in Figs. 3(b) and 3(c) are plotted in Figs. 6 and 7, respectively. The fields in Fig. 7 are more regular than other cases. Though the crystal shown in Fig. 3(c) has hexagonal symmetry, its electric fields show again some hidden details of crystal disordering. In an ideal case, heights of peaks are the same, which is in contrast to the scenario in Fig. 7. This means that the crystal shown in Fig. 3(c) is not completely ideal, although, it is nearly ideal.

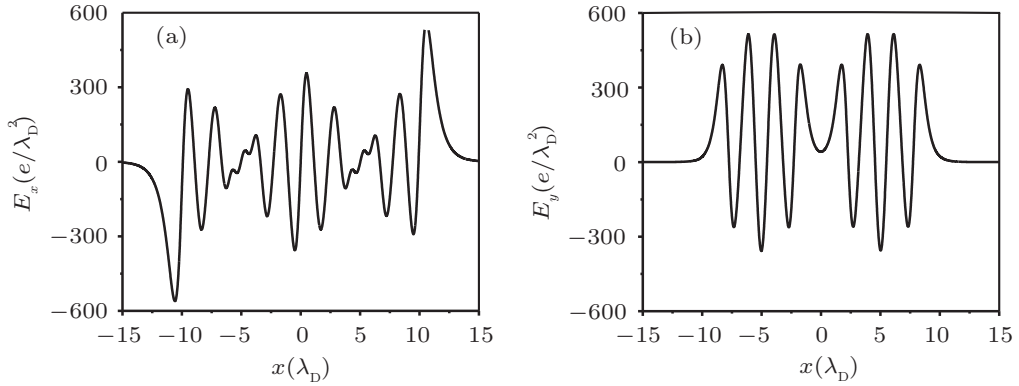


Fig. 6. (a) Longitudinal and (b) transverse electric fields in the middle of the crystal shown in Fig. 3(b) (at $y = 0$). Notice that there are two grains at $x = 0$ in Fig. 3(b).

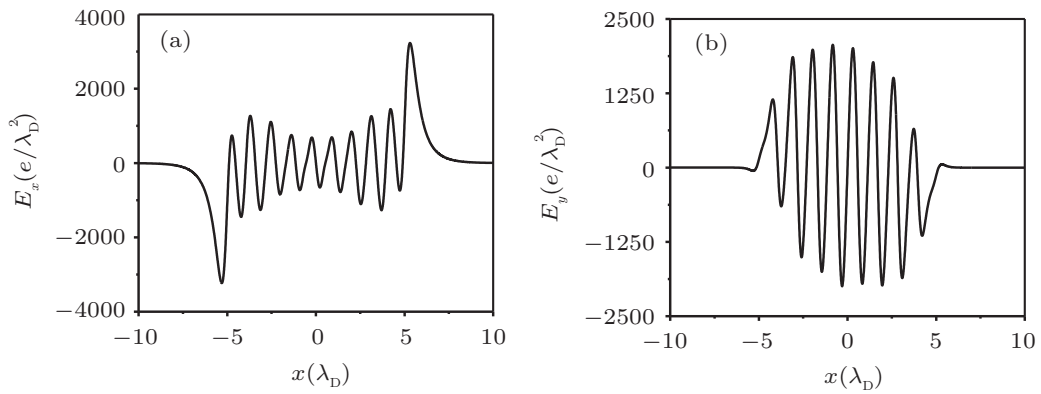


Fig. 7. (a) Longitudinal and (b) transverse electric fields in the middle of the crystal shown in Fig. 3(c) (at $y = 0$). This figure shows one of the best regular fields, which reflects the regularity of grain positions and good hexagonal structure.

Another thing is that grains have small oscillations, and so, all fields are momentary. We cannot produce 100% perfect crystals.

Finally, figure 8 shows fields of the crystal shown in Fig. 4. Unlike ideal situations, by moving toward the crystal center, the amplitude of the longitudinal electric field decreases and the amplitude of the transverse electric field increases. Moreover, the frequency of the longitudinal electric field is equal to the frequency of the transverse electric field. The reason as mentioned above is that the grains in the top row are not between grains in the bottom row.

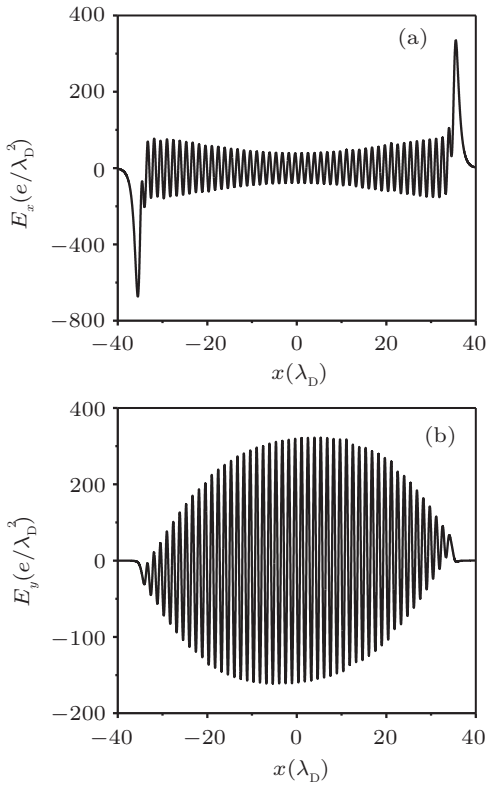


Fig. 8. (a) Longitudinal and (b) transverse electric fields in the middle of the crystal shown in Fig. 4 (at $y = 0$).

4. Conclusions

We report molecular dynamics simulations of 2D complex plasma crystals with arbitrary shapes. A rigid walls assumption is used; it is especially suitable for right-angle crystals. Two-row crystals are produced with this simple and new method. It is the second method of simulating the two-row crystals and the first method is explained in our previous work.[24]

The parameters that have influence on inside structures of crystals are obtained. These parameters are the number of grains, grains charge, length and width of the crystal. We can prognosticate the internal structure of a crystal: square, hexagonal, or something else. In right-angle crystals, by increasing n, q, and b the number of grain rows increases and by increasing a the number of rows decreases. It is shown that boundary effects are of short range and boundaries do not change the internal structure usually.

We report long and narrow crystals that are a good candidate for electrostatic wigglers in FELs. Production of ideal crystals are complex and even in the computer, we can achieve the ideal two-row crystals approximately. Any little disordering at the grain position leads to a large irregularity in electric field. The electric field components E_x and E_y show the hidden details of these disorderings and also asymmetries that cannot be seen from grain positions.

References

[1] Vladimirov S V and Samarian A A 2007 *Plasma Phys Control Fusion* **49** B95
[2] Genzel R 2006 *Annual MPE Report 293* (Munich: Max-Planck-Institut für extraterrestrische Physik)
[3] Shukla P K and Mamun A A 2001 *Introduction to dusty plasma physics* (Bristol: Institute of Physics Publishing)
[4] Feng Y, Goree J and Liu B 2010 *Phys. Rev. E* **82** 036403
[5] Sodha M S 2014 *Kinetics of complex plasmas* (New Delhi: Springer)
[6] Hartmann P, Donkó I and Donkó Z 2013 *Rev. Sci. Instrum.* **84** 023501
[7] Thompson C , O'angelo N and Merlino R L 1999 *Phys. Plasmas* **6** 1421
[8] Heijmans L C J and Nijdam S 2016 *Phys. Plasmas* **23** 043703
[9] Schmidt C and Piel A 2016 *Phys. Plasmas* **23** 083704
[10] Vladimirov S V, Ostrikov K and Samarian A A 2005 *Physics and applications of complex plasmas* (London: Imperial College Press)
[11] Shahzad A and He M G 2016 *Phys. Plasmas* **23** 093708
[12] Haralson Z and Goree J 2016 *Phys. Plasmas* **23** 093703
[13] Ishihara O 2007 *J. Phys. D: Appl. Phys.* **40** R121
[14] Coëdel L, Nosenko V, Ivlev A V, Zhdanov S K, Thomas H M and Morfill G E 2010 *Phys. Rev. Lett.* **104** 195001
[15] Hartmann P, Rosenberg M, Kalman G J and Donkó Z 2011 *Phys. Rev. E* **84** 016409
[16] Nosenko V, Ivlev A V and Morfill G E 2013 *Phys. Rev. E* **87** 043115
[17] Petrov O F, Vasiliev M M, Vaulina O S, Stacenko K B, Vasilieva E V, Lisin E A, Tun Y and Fortov V E 2015 *Europhys. Lett.* **111** 45002
[18] Bonitz M, Horing N and Ludwig P 2010 *Introduction to complex plasmas*, Vol. 59 (Cham: Springer)
[19] Liu Y H, Chew L Y and Yu M Y 2008 *Phys. Rev. E* **78** 066405
[20] Zhdanov S K, Thoma M H, Knapek C A and Morfill G E 2012 *New J. Phys.* **14** 023030
[21] Puttscher M and Melzer A 2014 *New J. Phys.* **16** 043026
[22] Reichstein T, Wilms J and Piel A 2013 *IEEE Trans. Plasma Sci.* **41** 759
[23] Djouder M, Kermoun F, Mitiche M D and Lamrous O 2016 *Phys. Plasmas* **23** 013701
[24] Bahadory B and Mirzanejhad S 2011 *Phys. Scripta* **84** 035501
[25] Huang F, Liu Y H, Chen Z Y, Wang L and Ye M F 2013 *Chin. Phys. Lett.* **30** 115201
[26] Yan J, Feng F, Liu F, Dong L and He Y 2016 *Chin. Phys. B* **25** 095202
[27] Yan J, Feng F, Liu F C and He Y F 2017 *Chin. Phys. B* **26** 095202
[28] Mirzanejhad S and Bahadory B 2007 *Phys. Plasmas* **14** 043101
[29] Fortov V, Iakubov I and Khrapak A 2006 *Physics of strongly coupled plasma*, Vol. 135 (Oxford: Oxford University Press)
[30] Saitou Y, Nakamura Y, Kamimura T and Ishihara O 2012 *Phys. Rev. Lett.* **108** 065004
[31] Liu B and Goree J 2014 *Phys. Rev. E* **89** 043107
[32] Joyce G, Lampe M and Ganguli G 2001 *IEEE Trans. Plasma Sci.* **29** 238
[33] Piel A and Wilms J 2016 *Phys. Plasmas* **23** 073701